A unified theory for dark matter halo mass function and density profile

Zhijie (Jay) Xu[1, *]

[1] *Physical and Computational Sciences Directorate, Pacific Northwest National Laboratory, Richland, WA 99352, USA*

Halo abundance and structures are critical to understand the small scale challenges for ΛCDM cosmology. We present a unified theory and analytical models for both halo mass function and halo density profile based on a random walk of halos and dark matter particles. The position dependent waiting time in random walk leads to a stretched Gaussian for mass function and density with a power-law on small scale and an exponential decay on large scale. Both Press-Schechter mass function and Einasto density profile can be easily recovered. This new perspective provides a simple theory for universal halo mass function and density profile.

Introduction.— Within the standard ΛCDM (cold dark matter) cosmology [1–4], the formation of structures proceeds hierarchically with small structures coalescing into large structures in a "bottom-up" fashion. For system with long-range interaction, the formation of halos of different size is necessary to maximize system entropy [5]. Therefore, highly localized halo structures and their evolution are major features of ΛCDM model [6, 7]. As a counterpart of "eddies" in hydrodynamic turbulence, "halos" are the building blocks in the flow of dark matter [8]. Halo abundance and internal structure play a central role for modeling of structure formation and evolution. The two quantities are also critical to understand the small scale challenges for ΛCDM when comparing model with observations [9–12]. However, despite having been extensively studied over many decades, our understanding is still not entirely satisfactory.

First, the abundance of dark matter halos is described by a halo mass function. The seminal Press-Schechter (PS) model allows one to predict the shape and evolution of mass function [13]. This model relies on a threshold value of overdensity (δ_c) that can be obtained from the nonlinear collapse of a spherical over-density [14, 15]. Bond et al. provided an alternative derivation using an excursion set approach (EPS) that puts the theory on a firmer footing by removing the fudge factor in original PS model [16]. However, when compared to N-body simulations, both PS and EPS models overestimate the number of low-mass halos and underestimate the number of massive halos. There are also significant errors at high redshifts [17]. Further improvement was achieved by computing the density threshold for ellipsoidal collapse [18, 19]. In contrast to the spherical collapse where the threshold δ_c is independent of the mass scale, the ellipsoidal collapse leads to a mass-dependent overdensity threshold. This modification (hereafter ST) considerably complicates the original model derivation but provieds a better agreement with simulations.

Because of its simplicity, the PS-EPS-ST mass functions are still the only and the most popular analytic models. However, the theoretical basis of this approach is at best heuristic. First, the derivation requires a threshold overdensity from a simplified (if not over simplified) collapse model (either spherical or ellipsoidal). Second, the linear density field is required to identify collapsed structures that is deeply in the non-linear regime. Finally, a specific smoothing filter (the sharp k-space filter) is required for the random walk of a local overdensity. In principle, halo mass function should be an objective and intrinsic property of self-gravitating collisionless system that is independent of the choice of collapse models or smoothing filters. In this letter, a different approach is taken to derive the halo mass function based on the random walk of halos in mass space, which is a direct result of the inverse mass cascade in dark matter flow [20].

Next, the structure of halos is described by the halo density profile [21] that can be studied both analytically and numerically with N-body simulations [22, 23]. Since the seminal work of spherical collapse [15], the power-law density profile was derived under the self-similar approximation. The secondary infall model suggests a power-law density dependent on the initial density of the region that collapsed [24, 25]. High-resolution N-body simulations have shown nearly universal profile with a cuspy density shallower than isothermal profile at smaller radius and steeper at larger radius [26, 27]. For the cuspy inner density from simulations, there seems no consensus on the exact value of the asymptotic logarithmic density slope γ. Since the first prediction of $\gamma = -1.0$ in NFW profile [26], the inner density slope of simulated halos have different values from $\gamma > -1.0$ [28] to $\gamma = -1.2$ [29], and $\gamma \approx -1.3$ [30–32]. When compared with observations, the predicted cuspy density are consistently steeper [33–36], i.e. the cusp-core problem. After many years of study, there still lacks a complete understanding for the origin of nearly universal density profile [7]. In this letter, an entirely new approach is presented based on the random walk of dark matter particles, which provides an alternative theory for the universal halo structure.

Existing mass functions.— For comparison with our model, a brief overview of existing mass functions is presented. When a normalized variable $\nu = \delta_c^2/\sigma_\delta^2(m_h)$ is introduced, the PS mass function simply reads

$$f_{PS}(\nu) = \frac{1}{\sqrt{2\pi}\sqrt{\nu}} e^{-\nu/2}, \tag{1}$$

* zhijie.xu@pnnl.gov

where $\sigma_\delta^2(m_h)$ is the density fluctuation when density field is smoothed at halo mass scale m_h. The modified PS model (ST model) can be compactly written as:

$$f_{ST}(\nu) = A\sqrt{\frac{2q}{\pi}}\left(1+\frac{1}{(q\nu)^p}\right)\frac{1}{2\sqrt{\nu}}e^{-q\nu/2}, \quad (2)$$

where the normalization condition requires:

$$A = \frac{\sqrt{\pi}}{\Gamma(1/2)+2^{-p}\Gamma(1/2-p)}. \quad (3)$$

The best fitted parameters from simulation is $A = 0.3222$, $q = 0.75$, and $p = 0.3$ [37]. Both models satisfy the normalization condition $\int_0^\infty f(\nu)\,d\nu = 1$.

Many empirical mass functions were also proposed by fitting to the high-resolution simulation data [38–41]. For example, a universal mass function by Jenkins etc. (hereafter JK) covers a wide range of different cosmologies and redshifts that is written as [42],

$$f_{JK}(\nu) = \frac{0.315}{2\nu}\exp[-\left|\ln\left(\sqrt{v}/\delta_c\right)+0.61\right|^{3.8}], \quad (4)$$

where the threshold density $\delta_c = 1.6865$. It should be noted that these empirical mass functions might not satisfy the normalization constraint and can be difficult to extrapolate beyond the range of fit.

Simulation.— The numerical halo mass function for this work was generated from N-body simulations carried out by the Virgo consortium. A comprehensive description can be found in [43, 44]. The same set of simulation data has been widely used in studies from clustering statistics [44] to the formation of halo clusters in large scale environments [45], and testing models for halo abundance and mass functions [18]. Two relevant datasets from this N-boby simulation, i.e. halo-based and correlation-based statistics of dark matter flow, can be found at Zenodo.org [46, 47], along with the accompanying slides, "A comparative study of dark matter flow & hydrodynamic turbulence and its applications" [8]. All data files are also available on GitHub [48].

Double-λ halo mass function.— In CDM cosmology, halos are continuously merging with small structures (mass accretion). This facilitates an inverse mass cascade in halo mass space, i.e. a continuous mass transfer from small to large mass scales ("inverse") to allow structure formation. Small halos simply pass their mass onto larger and larger halos until a critical mass scale m_h^* defined as $\sigma_\delta^2(m_h^*) = \delta_c$. This process is local in mass space, two-way (forward/backward), asymmetric (forward is dominant over backward), and generally involves two regimes, i.e. propagation and termination [20]. The propagation range for halos with a mass $m_h < m_h^*$ involves a sequence of merging with single mergers (the smallest structure) to propagate mass to larger mass scales. In this range, the rate of mass transfer ε_m is independent of halo mass. The termination stage ($m_h > m_h^*$) involves the consumption (deposition) of mass cascaded from scales below m_h^* to grow halos above m_h^*, i.e. the deposition range.

Based on this description, inverse mass cascade can be further refined into random walk of halos in mass space. Halos are migrating in mass space by merging with or losing single mergers. For halos at a given mass, there exists a waiting time τ_g (or jumping frequency) for halos to migrate from that given mass to neighboring mass. Different from standard random walk with a constant waiting time, the halo waiting time τ_g is dependent on the mass of halo, i.e. a position-dependent τ_g. This is because the waiting time should be inversely proportional to the surface area of halos. The larger halo surface area S_h, the more chances to merge with or lose single mergers, and the shorter waiting time τ_g. For halos with a given mass m_h, the waiting time $\tau_g \propto m_h^{-\lambda}$, where λ is a key halo geometry parameter. Intuitively, $\lambda \approx 2/3$ (i.e. $S_h \propto m_h^{2/3}$) for large halos in deposition range with low concentration, whose central structure are still dynamically adjusted due to fast mass accretion. While for small halos with high concentration (propagation range), the mass accretion is slow and inner structure is stable [49]. These halos are fractal objects with a fractal surface dimension $2 < D_h \leq 3$. Parameter $\lambda = D_h/3$ can be greater than 2/3 (see Eq. (26)). Therefore, two different λ values (i.e. double-λ) are required for two regimes.

For a power-law waiting time, the random walk of halos in mass space reads (Langevin equation)

$$\frac{\partial m_h(t)}{\partial t} = \sqrt{2D_p(m_h)}\varsigma(t), \quad (5)$$

where the position-dependent diffusivity reads

$$D_p(m_h) = D_{p0}(t)m_h^{2\lambda}. \quad (6)$$

Here $D_{p0}(t)$ is a proportional constant for diffusivity D_p. The white Gaussian noise $\varsigma(t)$ satisfies the covariance $\langle\varsigma(t)\varsigma(t')\rangle = \delta(t-t')$ with a zero mean $\langle\varsigma(t)\rangle = 0$. Equation (5) describes the stochastic evolution of halo mass m_h with waiting time $\tau_g(m_h) \propto m_h^{-\lambda}$.

In Stratonovich interpretation [50], the Langevin equation (Eq. (5)) yields to a distribution $P_h(m_h,t)$ satisfying the corresponding Fokker-Planck equation

$$\frac{\partial P_h(m_h,t)}{\partial t} = D_{p0}\frac{\partial}{\partial m_h}\left[m_h^\lambda\frac{\partial}{\partial m_h}\left(m_h^\lambda P_h(m_h,t)\right)\right], \quad (7)$$

which describes the probability of a halo with a given mass m_h in mass space. Obviously, the halo mass function $f_M(m_h,t)$ is exactly the distribution function P_h, i.e. $f_M \equiv P_h$. The solution to Eq. (7) is a stretched Gaussian that has an exponential cut-off for large m_h and a power-law behavior for small m_h,

$$f_M(m_h,t) = \frac{m_h^{-\lambda}}{\sqrt{\pi D_{p0}t}}\exp\left[-\frac{m_h^{2-2\lambda}}{4(1-\lambda)^2 D_{p0}t}\right]. \quad (8)$$

The mean square displacement in mass space is

$$\begin{aligned}\langle m_h^2\rangle &= \int_0^\infty f_M(m_h,t)\,m_h^2 dm_h \\ &= \frac{1}{\sqrt{\pi}}\Gamma\left(\frac{3-\lambda}{2-2\lambda}\right)\left[4(1-\lambda)^2 D_{p0}t\right]^{\frac{1}{1-\lambda}} \equiv \gamma_0 m_h^{*2}.\end{aligned} \quad (9)$$

where $m_h^*(t)$ is the critical mass scale and γ_0 is just a proportional constant. With the exponent of $1/(1-\lambda) \geq 1$ in Eq. (9), it is clear that the random walk of halos in mass space is a super-diffusion. Solution of $f_M(m_h, t)$ (Eq. (8)) can be rewritten in terms of m_h^*,

$$f_M(m_h,t) = \frac{(1-\lambda)}{m_h^*\sqrt{\pi\eta_0}} \left(\frac{m_h^*}{m_h}\right)^{\lambda} \exp\left[-\frac{1}{4\eta_0}\left(\frac{m_h}{m_h^*}\right)^{2-2\lambda}\right], \tag{10}$$

where the dimensionless constant η_0

$$\eta_0 = \frac{1}{4}\left[\frac{\gamma_0\sqrt{\pi}}{\Gamma\left((3-\lambda)/(2-2\lambda)\right)}\right]^{1-\lambda}. \tag{11}$$

The time dependence of f_M is absorbed into m_h^*. This is only possible when statistically steady state is established with a scale-independent rate of mass transfer ε_m in mass cascade [20]. Since geometry parameter λ can be dependent on mass scale and varying in [2/3, 1], the mass function in Eq. (10) can be naturally generalized to a double-λ mass function with λ_1 for propagation range and λ_2 for deposition range,

$$f_M(m_h,a) = (2\sqrt{\eta_0})^{-q}\frac{2(1-\lambda_1)}{q\Gamma(q/2)} \cdot \left(\frac{m_h^*}{m_h}\right)^{\lambda_1}\frac{1}{m_h^*}\exp\left[-\frac{1}{4\eta_0}\left(\frac{m_h}{m_h^*}\right)^{2-2\lambda_2}\right]. \tag{12}$$

By introducing $\nu = (m_h/m_h^*)^{2/3}$, the three parameter double-λ mass function can be finally written as,

$$f_{D\lambda}(\nu) = \frac{p\left(2\sqrt{\eta_0}\right)^{-q}}{\Gamma(q/2)}\nu^{\frac{pq}{2}-1}\exp\left(-\frac{\nu^p}{4\eta_0}\right), \tag{13}$$

where model parameters p and q have a clear physical meaning related to geometry parameters λ_1 and λ_2,

$$p = 3(1-\lambda_2) \quad \text{and} \quad q = \frac{(1-\lambda_1)}{(1-\lambda_2)}. \tag{14}$$

Clearly, Eq. (13) reduces to Press-Schechter (PS) mass function if $\lambda_1 = \lambda_2 = 2/3$, $\eta_0 = 1/2$. However, the double-λ halo mass function does not rely on any collapse model (spherical or ellipsoidal). Current formulation takes an entirely different approach based on the random walk of halos in mass space. The critical overdensity δ_c from spherical or elliptical collapse model is not required in this formulation. The halo geometry exponent λ has a fundamental meaning to relate halo surface area to its mass. The cosmology and redshift dependence of λ_1 and λ_2 can be systematically studied by fitting model to the simulation data, similar to the study in [40, 41]. Figure 1 plots different mass functions compared with simulation data. The best fit to the simulation data gives values of $\eta_0 = 0.76$, $q = 0.556$, and $p = 1$. We can estimate $\lambda_1 = 0.815$ in propagation range and $\lambda_2 = 2/3$ in deposition range. The double-λ mass function matches the simulation data for the entire range of halo mass.

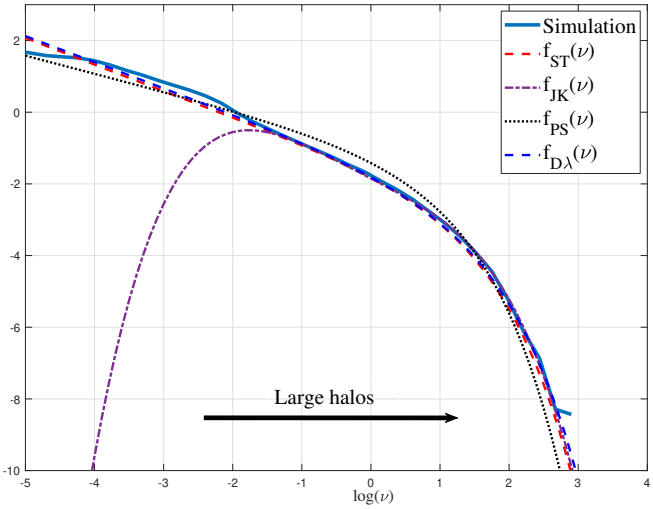

FIG. 1. Comparison between different mass functions (log(f(ν))) and simulation data at z=0. The PS mass function underestimates the mass in large halos. The fitted JK mass function matches simulation only in a given range. The double-λ mass function (Eq. (13)) matches both simulation and ST mass function for entire range.

Alternatively, similar to the scale radius r_s for halo density, we may introduce a scale mass m_{hs} where logarithmic slope $\partial\log(f_M)/\partial\log(m_h) = -1$ such that $m_{hs} = (2\eta_0 q)^{3/(2p)} m_h^*$ from Eq. (12). With a new scaled variable $\bar{\nu} = (m_h/m_{hs})^{2/3}$, mass function in Eq. (13) can be further simplified to have only two-parameters p and q,

$$f_{D\lambda}(\bar{\nu}) = \frac{p(q/2)^{q/2}}{\Gamma(q/2)}\bar{\nu}^{\frac{pq}{2}-1}\exp\left(-\frac{q}{2}\bar{\nu}^p\right). \tag{15}$$

Double-γ halo density profile.— The halo density profile can be derived based on a similar idea. To find the halo density, we need to derive the particle distribution function from the random walk of dark matter particles. This shares similarity with deriving the diffusion equation from standard Brownian motion. The random walk of dark matter particle in 3D space can be described by a Langevin equation for particle position $\boldsymbol{X}_t$,

$$\frac{d\boldsymbol{X}_t}{dt} = \sqrt{2D_P(\boldsymbol{X}_t)}\boldsymbol{\xi}(t). \tag{16}$$

When we follow the mass accretion of a halo, the waiting time $\tau_g \propto m_h^{-\lambda}$. Similarly, the waiting time of particle random walk should also be a function of position

$$\tau_p(r) \propto m_r(r)^{-\lambda} \propto r^{-\gamma}, \tag{17}$$

such that the position-dependent diffusivity reads

$$D_P(\boldsymbol{X}_t) = D_0(t)r^{2\gamma}, \tag{18}$$

where $D_0(t)$ is a proportional constant. Here scale $r = \sqrt{\boldsymbol{X}_t \cdot \boldsymbol{X}_t}$ is the radial distance from the center of halo, and $m_r(r)$ is the halo mass enclosed in scale r. The

corresponding 3D Fokker-Planck equation in Cartesian coordinate can be directly obtained for particle distribution function $P_r(\boldsymbol{X},t)$,

$$\frac{\partial P_r(\boldsymbol{X},t)}{\partial t} = D_0 \frac{\partial}{\partial X_i}\left[r^\gamma \frac{\partial}{\partial X_i}\left(r^\gamma P_r(\boldsymbol{X},t)\right)\right]. \quad (19)$$

The corresponding solution in spherical coordinate is

$$P_r(r,t) = \frac{(1-\gamma)r^{-\gamma}\exp\left(-\frac{r^{2-2\gamma}}{4(1-\gamma)^2 D_0 t}\right)}{2\pi\left[4(1-\gamma)^2 D_0 t\right]^{\frac{3-\gamma}{2-2\gamma}}\Gamma\left(\frac{3-\gamma}{2-2\gamma}\right)}. \quad (20)$$

Similarly, the exponent γ can be different for halos below and above the critical mass m_h^*. By using two different γ for r dependence of waiting time $\tau_p(r) \propto r^{-\gamma}$, i.e. γ_1 and γ_2 for propagation and deposition ranges, we have

$$P_r(r,t) = \frac{(1-\gamma_2)r^{-\gamma_1}\exp\left(-\frac{r^{2-2\gamma_2}}{4(1-\gamma_2)^2 D_0 t}\right)}{2\pi\left[4(1-\gamma_2)^2 D_0 t\right]^{\frac{3-\gamma_1}{2-2\gamma_2}}\Gamma\left(\frac{3-\gamma_1}{2-2\gamma_2}\right)}. \quad (21)$$

Introducing the conventional scale radius $r_s(t)$ where the logarithmic slope of $P_r(r,t)$ equals -2, we should have

$$4(1-\gamma_2)^2 D_0 t = \frac{2-2\gamma_2}{2-\gamma_1} r_s^{2-2\gamma_2}. \quad (22)$$

Substituting Eq. (22) into Eq. (21) and introducing a dimensionless spatial-temporal variable $x = r/r_s(t)$,

$$P_r(x) = \frac{(1-\gamma_2)x^{-\gamma_1}\exp\left(-\frac{(2-\gamma_1)x^{2-2\gamma_2}}{2-2\gamma_2}\right)}{2\pi\Gamma\left(\frac{3-\gamma_1}{2-2\gamma_2}\right)\left[\frac{2-2\gamma_2}{2-\gamma_1}\right]^{\frac{3-\gamma_1}{2-2\gamma_2}}}. \quad (23)$$

Finally, the two parameter particle distribution function can be written in a very simple form (similar to halo mass function in Eq. (15))

$$P_r(x) = \frac{\alpha\beta^{-(\frac{1}{\alpha}+\frac{1}{\beta})}}{4\pi\Gamma\left(\frac{1}{\alpha}+\frac{1}{\beta}\right)} x^{\frac{\alpha}{\beta}-2}\exp\left(-\frac{x^\alpha}{\beta}\right), \quad (24)$$

where two dimensionless parameters α and β are

$$\alpha = 2-2\gamma_2 \quad \text{and} \quad \beta = \frac{2-2\gamma_2}{2-\gamma_1}. \quad (25)$$

The time dependence of halo density is absorbed into the scale radius $r_s(t)$. The double-γ distribution function reduces to the Einasto profile with $\alpha = 2\beta$. The cumulative distribution in spherical coordinate can be easily obtained as,

$$\int_0^x P_r(y)\,4\pi y^2 dy = 1 - \frac{\Gamma\left(\frac{1}{\alpha}+\frac{1}{\beta}, \frac{x^\alpha}{\beta}\right)}{\Gamma\left(\frac{1}{\alpha}+\frac{1}{\beta}\right)}, \quad (26)$$

where $\Gamma(x,y)$ is an upper incomplete gamma function. Both halo mass function and halo density profile can be analytically derived based on the inverse mass cascade.

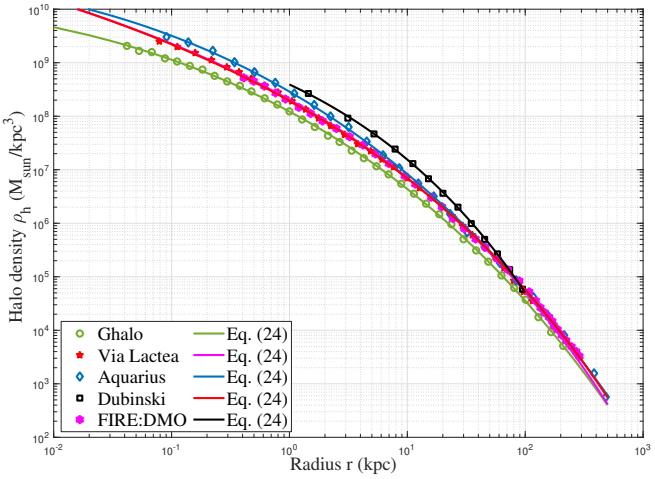

FIG. 2. Halo density profiles for simulated halos: 1) Ghalo [52]; 2) Via Lactea [53]; 3) Aquarius [54]; 4) Dubinski [55]; 5) FIRE:DMO [31]. The double-γ density model (Eq. (24)) was also used to fit all simulated halos for the entire range of r.

Here we provide a clear physical origin of halo density. The complete halo density profile can be finally written as $\rho_h(r,t) = \rho_c(t)P_r(x)$, where $\rho_c(t)$ is a scale of density. Figure 2 provides the density profiles of some simulated halos, with best fit by our proposed model in Eq. (24). The relation between λ and γ might be obtained from the theory of energy cascade. Similar to the mass cascade in propagation range, there exist an inverse energy cascade from small to large scales with a constant rate ε_u that is independent of both scale r and time. In this range, the small scale structures evolve very fast and do not feel the slow evolving large scales directly except through ε_u and G. This description indicates that relevant quantities in this range should be determined by and only by ε_u (m^2/s^3), gravitational constant G ($m^3/kg\cdot s^2$), and scale r [51]. By a simple dimensional analysis, the halo mass enclosed within scale r should follow

$$m_r(r) \propto \varepsilon_u^{2/3} G^{-1} r^{5/3}, \quad (27)$$

such that $\gamma_1 = 5\lambda_1/3$ (see Eq. (17)). With $\lambda_1 \approx 4/5$ from Fig. 1, we would expect $\gamma_1 = 4/3$, which is the limiting density slope for fully virialized halos.

Conclusion.— In this letter, we present a simple theory for halo mass function based on the random walk of halos in mass space. The position-dependent waiting time $\tau_g \propto m_h^{-\lambda}$ leads to an analytical mass function modelled by a stretched Gaussian with a power-law behavior on small scale and exponential decay on large scale. This can be further improved by considering a mass-dependent λ, i.e. a double-λ mass function in Eq. (13). Similarly, a double-γ halo density profile is proposed based on the random walk of dark matter particles with a position-dependent waiting time $\tau_g \propto r^{-\gamma}$ (Eq. (24)). The Press-Schechter mass function and Einasto profile are just special cases. Therefore, a unified theory is presented for universal halo mass function and density profile.

[1] P. J. E. Peebles, "Tests of cosmological models constrained by inflation," The Astrophysical Journal **284**, 439–444 (1984).

[2] D. N. Spergel, L. Verde, H. V. Peiris, E. Komatsu, M. R. Nolta, C. L. Bennett, M. Halpern, G. Hinshaw, N. Jarosik, A. Kogut, M. Limon, S. S. Meyer, L. Page, G. S. Tucker, J. L. Weiland, E. Wollack, and E. L. Wright, "First-Year Wilkinson Microwave Anisotropy Probe (WMAP) Observations: Determination of Cosmological Parameters," The Astrophysical Journal Supplement Series **148**, 175–194 (2003), arXiv:astro-ph/0302209 [astro-ph].

[3] E. Komatsu, K. M. Smith, J. Dunkley, C. L. Bennett, B. Gold, G. Hinshaw, N. Jarosik, D. Larson, M. R. Nolta, L. Page, D. N. Spergel, M. Halpern, R. S. Hill, A. Kogut, M. Limon, S. S. Meyer, N. Odegard, G. S. Tucker, J. L. Weiland, E. Wollack, and E. L. Wright, "Seven-year Wilkinson Microwave Anisotropy Probe (WMAP) Observations: Cosmological Interpretation," The Astrophysical Journal Supplement Series **192**, 18 (2011), arXiv:1001.4538 [astro-ph.CO].

[4] C. S. Frenk and S. D. M. White, "Dark matter and cosmic structure," Annalen der Physik **524**, 507–534 (2012), arXiv:1210.0544 [astro-ph.CO].

[5] Zhijie Xu, "The maximum entropy distributions of velocity, speed, and energy from statistical mechanics of dark matter flow," arXiv e-prints , arXiv:2110.03126 (2021).

[6] J. Neyman and E. L. Scott, "A theory of the spatial distribution of galaxies," Astrophysical Journal **116**, 144–163 (1952).

[7] A. Cooray and R. Sheth, "Halo models of large scale structure," Physics Reports-Review Section of Physics Letters **372**, 1–129 (2002).

[8] Zhijie Xu, "A comparative study of dark matter flow & hydrodynamic turbulence and its applications," (2022).

[9] Ricardo A. Flores and Joel R. Primack, "Observational and Theoretical Constraints on Singular Dark Matter Halos," The Astrophysical Journal Letters **427**, L1 (1994), arXiv:astro-ph/9402004 [astro-ph].

[10] W. J. G. de Blok, "The Core-Cusp Problem," Adv. Astron. **2010**, 789293 (2010), arXiv:0910.3538 [astro-ph.CO].

[11] Anatoly Klypin, Andrey V. Kravtsov, Octavio Valenzuela, and Francisco Prada, "Where are the missing galactic satellites?" The Astrophysical Journal **522**, 82–92 (1999).

[12] Michael Boylan-Kolchin, James S. Bullock, and Manoj Kaplinghat, "Too big to fail? the puzzling darkness of massive milky way subhaloes," Monthly Notices of the Royal Astronomical Society: Letters **415**, L40–L44 (2011).

[13] W. H. Press and P. Schechter, "Formation of galaxies and clusters of galaxies by self-similar gravitational condensation," Astrophysical Journal **187**, 425–438 (1974).

[14] K. Tomita, "Formation of gravitationally bound primordial gas clouds," Progress of Theoretical Physics **42**, 9 (1969).

[15] J. E. Gunn and J. R. Gott, "Infall of matter into clusters of galaxies and some effects on their evolution," Astrophysical Journal **176**, 1 (1972).

[16] J. R. Bond, S. Cole, G. Efstathiou, and N. Kaiser, "Excursion set mass functions for hierarchical gaussian fluctuations," Astrophysical Journal **379**, 440–460 (1991).

[17] V. Springel, S. D. M. White, A. Jenkins, C. S. Frenk, N. Yoshida, L. Gao, J. Navarro, R. Thacker, D. Croton, J. Helly, J. A. Peacock, S. Cole, P. Thomas, H. Couchman, A. Evrard, J. Colberg, and F. Pearce, "Simulations of the formation, evolution and clustering of galaxies and quasars," Nature **435**, 629–636 (2005).

[18] R. K. Sheth, H. J. Mo, and G. Tormen, "Ellipsoidal collapse and an improved model for the number and spatial distribution of dark matter haloes," Monthly Notices of the Royal Astronomical Society **323**, 1–12 (2001).

[19] R. K. Sheth and G. Tormen, "Large-scale bias and the peak background split," Monthly Notices of the Royal Astronomical Society **308**, 119–126 (1999).

[20] Zhijie Xu, "Inverse mass cascade in dark matter flow and effects on halo mass functions," arXiv e-prints , arXiv:2109.09985 (2021).

[21] A. Del Popolo and P. Kroupa, "Density profiles of dark matter haloes on galactic and cluster scales," Astronomy & Astrophysics **502**, 733–747 (2009).

[22] B. Moore, F. Governato, T. Quinn, J. Stadel, and G. Lake, "Resolving the structure of cold dark matter halos," Astrophysical Journal **499**, L5–+ (1998).

[23] A. Klypin, A. V. Kravtsov, J. S. Bullock, and J. R. Primack, "Resolving the structure of cold dark matter halos," Astrophysical Journal **554**, 903–915 (2001).

[24] E. Bertschinger, "Self-similar secondary infall and accretion in an einstein-desitter universe," Astrophysical Journal Supplement Series **58**, 39–66 (1985).

[25] J. A. Fillmore and P. Goldreich, "Self-similar gravitational collapse in an expanding universe," Astrophysical Journal **281**, 1–8 (1984).

[26] J. F. Navarro, C. S. Frenk, and S. D. M. White, "A universal density profile from hierarchical clustering," Astrophysical Journal **490**, 493–508 (1997).

[27] J. F. Navarro, E. Hayashi, C. Power, A. R. Jenkins, C. S. Frenk, S. D. M. White, V. Springel, J. Stade, and T. R. Quinn, "The inner structure of acdm haloes - iii. universality and asymptotic slopes," Monthly Notices of the Royal Astronomical Society **349**, 1039–1051 (2004).

[28] Julio F. Navarro, Aaron Ludlow, Volker Springel, Jie Wang, Mark Vogelsberger, Simon D. M. White, Adrian Jenkins, Carlos S. Frenk, and Amina Helmi, "The diversity and similarity of simulated cold dark matter haloes," Monthly Notices of the Royal Astronomical Society **402**, 21–34 (2010), https://academic.oup.com/mnras/article-pdf/402/1/21/18573804/mnras0402-0021.pdf.

[29] Jürg Diemand and Ben Moore, "The Structure and Evolution of Cold Dark Matter Halos," Advanced Science Letters **4**, 297–310 (2011), arXiv:0906.4340 [astro-ph.CO].

[30] F. Governato, C. Brook, L. Mayer, A. Brooks, G. Rhee, J. Wadsley, P. Jonsson, B. Willman, G. Stinson, T. Quinn, and P. Madau, "Bulgeless dwarf galaxies and dark matter cores from supernova-driven outflows," Nature **463**, 203–206 (2010).

[31] Daniel McKeown, James S. Bullock, Francisco J. Mercado, Zachary Hafen, Michael Boylan-Kolchin, Andrew Wetzel, Lina Necib, Philip F. Hopkins, and Sijie Yu, "Amplified J-factors in the Galactic Centre for velocity-

dependent dark matter annihilation in FIRE simulations," Monthly Notices of the Royal Astronomical Society **513**, 55–70 (2022), arXiv:2111.03076 [astro-ph.GA].

[32] Alexandres Lazar, James S Bullock, Michael Boylan-Kolchin, T K Chan, Philip F Hopkins, Andrew S Graus, Andrew Wetzel, Kareem El-Badry, Coral Wheeler, Maria C Straight, Dušan Kereš, Claude-André Faucher-Giguère, Alex Fitts, and Shea Garrison-Kimmel, "A dark matter profile to model diverse feedback-induced core sizes of ΛCDM haloes," Monthly Notices of the Royal Astronomical Society **497**, 2393–2417 (2020), https://academic.oup.com/mnras/article-pdf/497/2/2393/33571817/staa2101.pdf.

[33] W. J. G. de Blok and A. Bosma, "High-resolution rotation curves of low surface brightness galaxies," Astronomy & Astrophysics **385**, 816–846 (2002), arXiv:astro-ph/0201276 [astro-ph].

[34] W. J. G. de Blok, Albert Bosma, and Stacy McGaugh, "Simulating observations of dark matter dominated galaxies: towards the optimal halo profile," Monthly Notices of the Royal Astronomical Society **340**, 657–678 (2003), https://academic.oup.com/mnras/article-pdf/340/2/657/18649385/340-2-657.pdf.

[35] R. A. Swaters, B. F. Madore, F. C. van den Bosch, and M. Balcells, "The Central mass distribution in dwarf and low-surface brightness galaxies," Astrophys. J. **583**, 732–751 (2003), arXiv:astro-ph/0210152.

[36] Rachel Kuzio de Naray and Tobias Kaufmann, "Recovering cores and cusps in dark matter haloes using mock velocity field observations," Monthly Notices of the Royal Astronomical Society **414**, 3617–3626 (2011), https://academic.oup.com/mnras/article-pdf/414/4/3617/18715139/mnras0414-3617.pdf.

[37] R. K. Sheth and G. Tormen, "An excursion set model of hierarchical clustering: ellipsoidal collapse and the moving barrier," Monthly Notices of the Royal Astronomical Society **329**, 61–75 (2002).

[38] M. S. Warren, K. Abazajian, D. E. Holz, and L. Teodoro, "Precision determination of the mass function of dark matter halos," Astrophysical Journal **646**, 881–885 (2006).

[39] D. S. Reed, R. Bower, C. S. Frenk, A. Jenkins, and T. Theuns, "The halo mass function from the dark ages through the present day," Monthly Notices of the Royal Astronomical Society **374**, 2–15 (2007).

[40] Euclid Collaboration, T. Castro, A. Fumagalli, R. E. Angulo, S. Bocquet, S. Borgani, C. Carbone, J. Dakin, K. Dolag, C. Giocoli, P. Monaco, A. Ragagnin, A. Saro, E. Sefusatti, M. Costanzi, A. Amara, L. Amendola, M. Baldi, R. Bender, C. Bodendorf, E. Branchini, M. Brescia, S. Camera, V. Capobianco, J. Carretero, M. Castellano, S. Cavuoti, A. Cimatti, R. Cledassou, G. Congedo, L. Conversi, Y. Copin, L. Corcione, F. Courbin, A. Da Silva, H. Degaudenzi, M. Douspis, F. Dubath, C. A. J. Duncan, X. Dupac, S. Farrens, S. Ferriol, P. Fosalba, M. Frailis, E. Franceschi, S. Galeotta, B. Garilli, B. Gillis, A. Grazian, F. Gruppi, S. V. H. Haugan, F. Hormuth, A. Hornstrup, P. Hudelot, K. Jahnke, S. Kermiche, T. Kitching, M. Kunz, H. Kurki-Suonio, P. B. Lilje, I. Lloro, O. Mansutti, O. Marggraf, M. Meneghetti, E. Merlin, G. Meylan, M. Moresco, L. Moscardini, E. Munari, S. M. Niemi, C. Padilla, S. Paltani, F. Pasian, K. Pedersen, V. Pettorino, S. Pires, G. Polenta, M. Poncet, L. Popa, L. Pozzetti, F. Raison, R. Rebolo, A. Renzi, J. Rhodes, G. Riccio, E. Romelli, R. Saglia, D. Sapone, B. Sartoris, P. Schneider, G. Seidel, G. Sirri, L. Stanco, P. Tallada Crespí, A. N. Taylor, R. Toledo-Moreo, F. Torradeflot, I. Tutusaus, E. A. Valentijn, L. Valenziano, T. Vassallo, Y. Wang, J. Weller, A. Zacchei, G. Zamorani, S. Andreon, S. Bardelli, E. Bozzo, C. Colodro-Conde, D. Di Ferdinando, M. Farina, J. Graciá-Carpio, V. Lindholm, C. Neissner, V. Scottez, M. Tenti, E. Zucca, C. Baccigalupi, A. Balaguera-Antolínez, M. Ballardini, F. Bernardeau, A. Biviano, A. Blanchard, A. S. Borlaff, C. Burigana, R. Cabanac, A. Cappi, C. S. Carvalho, S. Casas, G. Castignani, A. Cooray, J. Coupon, H. M. Courtois, S. Davini, G. De Lucia, G. Desprez, H. Dole, J. A. Escartin, S. Escoffier, F. Finelli, K. Ganga, J. Garcia-Bellido, K. George, G. Gozaliasl, H. Hildebrandt, I. Hook, S. Ilić, V. Kansal, E. Keihanen, C. C. Kirkpatrick, A. Loureiro, J. Macias-Perez, M. Magliocchetti, R. Maoli, S. Marcin, M. Martinelli, N. Martinet, S. Matthew, M. Maturi, R. B. Metcalf, G. Morgante, S. Nadathur, A. A. Nucita, L. Patrizii, A. Peel, V. Popa, C. Porciani, D. Potter, A. Pourtsidou, M. Pöntinen, A. G. Sánchez, Z. Sakr, M. Schirmer, M. Sereno, A. Spurio Mancini, R. Teyssier, J. Valiviita, A. Veropalumbo, and M. Viel, "Euclid preparation. xxiv. calibration of the halo mass function in cdm cosmologies," arXiv e-prints (2022), 10.48550/ARXIV.2208.02174.

[41] Sebastian Bocquet, Katrin Heitmann, Salman Habib, Earl Lawrence, Thomas Uram, Nicholas Frontiere, Adrian Pope, and Hal Finkel, "The mira-titan universe. III. emulation of the halo mass function," The Astrophysical Journal **901**, 5 (2020).

[42] A. Jenkins, C. S. Frenk, S. D. M. White, J. M. Colberg, S. Cole, A. E. Evrard, H. M. P. Couchman, and N. Yoshida, "The mass function of dark matter haloes," Monthly Notices of the Royal Astronomical Society **321**, 372–384 (2001).

[43] C. S. Frenk, J. M. Colberg, H. M. P. Couchman, G. Efstathiou, A. E. Evrard, A. Jenkins, T. J. MacFarland, B. Moore, J. A. Peacock, F. R. Pearce, P. A. Thomas, S. D. M. White, and N. Yoshida., "Public release of n-body simulation and related data by the virgo consortium," arXiv:astro-ph/0007362v1 (2000), 10.48550/arXiv.astro-ph/0007362.

[44] A. Jenkins, C. S. Frenk, F. R. Pearce, P. A. Thomas, J. M. Colberg, S. D. M. White, H. M. P. Couchman, J. A. Peacock, G. Efstathiou, and A. H. Nelson, "Evolution of structure in cold dark matter universes," Astrophysical Journal **499**, 20 (1998).

[45] J. M. Colberg, S. D. M. White, A. Jenkins, and F. R. Pearce, "Linking cluster formation to large-scale structure," Monthly Notices of the Royal Astronomical Society **308**, 593–598 (1999).

[46] Zhijie Xu, "Dark matter flow dataset part i: Halo-based statistics from cosmological n-body simulation," (2022).

[47] Zhijie Xu, "Dark matter flow dataset part ii: Correlation-based statistics from cosmological n-body simulation," (2022).

[48] Zhijie Xu, "Dark matter flow dataset," (2022).

[49] D. H. Zhao, Y. P. Jing, H. J. Mo, and G. Borner, "Accurate universal models for the mass accretion histories and concentrations of dark matter halos," Astrophysical Journal **707**, 354–369 (2009).

[50] R. L. Stratonovich, "A new representation for stochastic

integrals and equations," SIAM Journal on Control **4**, 362–371 (1966).

[51] Zhijie Xu, "Universal scaling laws and density slope for dark matter halos from rotation curves and energy cascade," arXiv e-prints (2022), 10.48550/ARXIV.2209.03313.

[52] J. Stadel, D. Potter, B. Moore, J. Diemand, P. Madau, M. Zemp, M. Kuhlen, and V. Quilis, "Quantifying the heart of darkness with GHALO - a multibillion particle simulation of a galactic halo," Monthly Notices of the Royal Astronomical Society: Letters **398**, L21–L25 (2009).

[53] J. Diemand, M. Kuhlen, P. Madau, M. Zemp, B. Moore, D. Potter, and J. Stadel, "Clumps and streams in the local dark matter distribution," Nature **454**, 735–738 (2008).

[54] V. Springel, J. Wang, M. Vogelsberger, A. Ludlow, A. Jenkins, A. Helmi, J. F. Navarro, C. S. Frenk, and S. D. M. White, "The Aquarius Project: the subhaloes of galactic haloes," Monthly Notices of the Royal Astronomical Society **391**, 1685–1711 (2008), https://academic.oup.com/mnras/article-pdf/391/4/1685/4881147/mnras0391-1685.pdf.

[55] John Dubinski and R. G. Carlberg, "The Structure of Cold Dark Matter Halos," The Astrophysical Journal **378**, 496 (1991).